

Article

Digital Induction Motor Model Based on the Finite Element Method

Pavol Bozek ¹, Tibor Krenicky ^{2,*} and Vanessa Prajova ³¹ Institute of Production Technologies, Faculty of Materials Science and Technology in Trnava, Slovak University of Technology in Bratislava, 917 24 Trnava, Slovakia² Department of Technical Systems Design and Monitoring, Faculty of Manufacturing Technologies with a Seat in Prešov, Technical University of Košice, Bayerova 1, 080 01 Prešov, Slovakia³ Institute of Industrial Engineering and Management, Faculty of Materials Science and Technology, Slovak University of Technology in Bratislava, J. Bottu 25, 917 24 Trnava, Slovakia* Correspondence: tibor.krenicky@tuke.sk

Abstract: This article presents the design of a drive system for robots and manipulators, which is based on the finite element method of an induction motor. The design process involves constructing a computer-aided design (CAD) model of the induction motor, which enables the generation of design documentation and control programs for computer numerical control (CNC) tools for manufacturing motor parts or conducting further research. A CAD model is developed for performing a finite element analysis of the motor in the SolidWorks software based on the popular AIR63V2 motor. The design of the motor's housing, rotor, and stator is developed. Additionally, the electrical parameters of the motor are calculated using Ansys Electronic Suite—Maxwell RMxpert, utilizing the classical analytical theory of electrical machines and the equivalent magnetic circuit method. This takes into account such effects as the non-linearity of electrical steel, the non-sinusoidality of the magnetic flux in the gap, and the displacement of electric current in massive conductors. A complete model of an induction motor for research has been created, enabling the study of dependencies of speed and electromagnetic torque of an induction motor. The natural frequency of the rotor is calculated, which ranges from 922 Hz to 1015 Hz. The obtained values of calculations of natural oscillations of the CAD model of the motor can be used for motor diagnostics. Furthermore, the created project in the Ansys software can be utilized to design an induction motor with its own characteristics, optimized for specific tasks.

Keywords: induction drive; robots and manipulators; digital model; finite element method

Citation: Bozek, P.; Krenicky, T.; Prajova, V. Digital Induction Motor Model Based on the Finite Element Method. *Appl. Sci.* **2023**, *13*, 5124. <https://doi.org/10.3390/app13085124>

Academic Editor: DaeEun Kim

Received: 24 February 2023

Revised: 9 April 2023

Accepted: 17 April 2023

Published: 20 April 2023



Copyright: © 2023 by the authors. Licensee MDPI, Basel, Switzerland. This article is an open access article distributed under the terms and conditions of the Creative Commons Attribution (CC BY) license (<https://creativecommons.org/licenses/by/4.0/>).

1. Introduction

Electric motors are critical components in a variety of industrial applications, including electric vehicles, robotics, and aerospace systems. The development of efficient and accurate computer-aided design (CAD) models for electric motors is therefore essential for the design, analysis, and optimization of these systems. In recent years, considerable research effort has been dedicated to the development of CAD models for electric motors. Induction motors (IM) have gained popularity in robot and arm drives due to their high reliability, low cost, and lack of permanent magnets [1].

The Induction Machines Handbook [2] offers a practical and up-to-date treatment of complex issues related to IM necessary for design and testing in both constant and variable-speed drives (with power electronics). It contains industrial design and testing knowledge with numerous case studies to aid in the assimilation of new knowledge.

Advanced issues and subjects in electric machines are extensively covered in the book [3] from principles to applications and case studies, with ample graphical and numerical results. The latest knowledge with strong industrialization potential has been added to

this edition, including orthogonal models of multiphase AC machines and thermal finite element analysis of electric machines.

The monograph [4] provides an up-to-date overview of numerical field computational methods and, in particular, of the finite element method (FEM). Particular attention is paid to the practical use of the FEM in designing electric motors.

The monograph [5] describes promising technology with MATLAB/SIMULINK in electrical machines, addressing the concept of electromechanical energy conversion and exploring various electrical machines, special electrical machines, electrical drives, and their applications using MATLAB/SIMULINK. It also provides a condensed and extensive review of current trends and outcomes with the ultimate goal of emphasizing energy conversion and up-to-date electrical applications for engineering students.

Engineering analysis is a crucial aspect of modern investigations, and a correctly constructed CAD model is the basis for such analysis [6–9]. CAD/CAM systems are widely used for computer simulation of products with complex shapes, design documentation, generation of control programs for CNC machines, or internal research to determine product parameters before release [10,11]. Some of the commonly used CAD systems include AutoCAD, SolidWorks, Pro/Engineer, and Unigraphics [12]; however, specialized packages of numerical modeling lack advanced facilities for engineering analysis.

CAE systems such as Abaqus, Ansys, COSMOS, and Nastran enable qualitative simulation of systems of different physical natures and the study of their response to various external influences, including stress distribution, temperature, velocity, and electromagnetic fields [13,14]. Using such software helps determine various parameters of the object under study before developing the first prototypes, ultimately eliminating defects at the development stage and reducing the development cycle [15].

The study [16] is aimed at a static and dynamic simulation and optimization approach for an induction motor. The model is validated using experimental data and shows good agreement with the measured results. Another digital simulation model of motor drive is [17]. The model is shown to provide accurate results for both steady-state and transient analyses. Based on such results, hybrid CAD models for synchronous reluctance motors that combine a magnetic equivalent circuit models with a finite element model are validated using experimental data showing good agreement with the measured results.

A computational model analyzing dynamic response of an induction motor stability under load was presented in [18]. The model is validated using both simulation and experimental data and shows good agreement with the measured results. A comprehensive mathematical model that includes methodology for assessing rotor transient stability was proposed in [19]. The model is validated using both simulation and experimental data, showing good agreement with the measured results. The authors of [20] evaluate the performance of induction motor control models for specific conditions.

The study [21] presents a design optimization approach for an induction electric motor aimed for automotive applications. The models are compared on the base of their accuracy, computation time, and ease of use. The results show that the optimized design improves the performance of the motor in terms of torque and efficiency.

The authors of [22] discuss the design of methods enabling the identification of the standstill parameters of electric induction motors with a focus on their stability. The authors highlight the importance of detailed consideration of key features in the design process and provide examples of how particular models comparison can be used to optimize the performance of electric machines. The article [23] presents a design and optimization approach for electric motors using core loss model. The results show that the approach can be used to improve the performance of electric motors in terms of efficiency and torque. A comprehensive overview of the available software tools for electric motor design and simulation aimed at effective control is given in [24]. The effects of piezoelectric stator mounting position angle, stator–rotor contact contact materials, and preload on motor torque are analyzed by simulation and presented in [25], identifying efficient modeling techniques for electric motor analysis, including torque modelling by vector synthesis.

The disadvantages of the existing CAD model tools are the limited possibilities in terms of the functions used, which do not allow for a comprehensive study of the model in terms of mechanical, electrical, electromagnetic and temperature parameters. Despite the advancements in electric motor CAD modeling, there are still certain shortcomings that need to be addressed. One of the main limitations is the accuracy of the models, particularly for complex geometries and nonlinear materials. Another challenge is the computational cost of the models, which can be prohibitively expensive for large-scale systems. In addition, the lack of standardization in the development and validation of CAD models makes it difficult to compare results from different studies. Finally, the availability of accurate and reliable input data, such as material properties and boundary conditions, can also be a challenge in some cases.

The aim of the study is to establish the dependencies between the characteristics of an IM developed on the basis of a model approach. In order to achieve this objective the following tasks have to be completed:

1. The development of a mathematical model of an IM.
2. The development of a CAD model of an IM.
3. Carrying out a performance study of the developed IM.
4. Carrying out a finite element analysis of the CAD model of an IM.

2. Materials and Methods

Before designing and creating a prototype in the form of a motor parameterization bench, a CAD model was developed for a finite element analysis of the investigated drive in order to conduct IM research and develop a correct diagnostic system [26,27]. The IM AIR63V2 drive was chosen as the basis for this model, as it meets all the necessary specifications and is an excellent choice for the study. The CAD model was created based on the passport of the IM AIR63V2 and a real sample from which some non-critical dimensions were taken [28]. A schematic diagram of the information flow of the design of the IM is shown in Figure 1.

The initial aspect pertained to the stator housing's design, encompassing cooling ribs, feet, and boron, ultimately serving as the terminal box. Figure 2 shows a diagram of the information flow when designing an asynchronous motor.

The IM enclosure is demonstrated in Figure 3, while Figure 4 displays the IM's rotor and stator.

The rotor and stator, which are the working components of the IM, were designed first. Following that, the other enclosure elements necessary for providing power supply, motor cooling, and movement of the motor's working parts were designed. The parts were assembled and verified to ensure they matched their intended design. To reduce the cost of processing model data, the stator winding was not included in the 3D model. A sectional view of the IM is presented in Figure 5, while Figure 6 displays a 3D model of the AIR63V2 induction motor.

In Ansys Electronic Suite—Maxwell RMXprt, the electrical parameters of an induction motor (IM) can be calculated. Like any other motor, an IM is characterized by its power, supply voltage, current consumption, and connection type; however, many of the parameters listed in the motor data sheet are nominal without taking into account inaccuracies or assumptions.

The RMXprt program within the Ansys Electromagnetic Suite, a part of the Maxwell complex, can be used to calculate the electrical parameters of the IM AIR 63V2 motor. This calculation utilizes classical analytical theory of electrical machines and the equivalent magnetic circuit method. It takes into account various effects, such as the non-linearity of electrical steel, non-sinusoidal magnetic flux in the gap, and current displacement in massive conductors.

One of the advantages of this program is the ability to modify parameters during the entire calculation process, allowing for the comparison of different characteristics with different initial data to obtain the optimal values [29].

To handle more extensive calculations, the setup established in RMxpert can be transformed into a Maxwell model, which employs the finite element method (FEM) to precisely evaluate static, harmonic electromagnetic and electric fields, as well as transients.

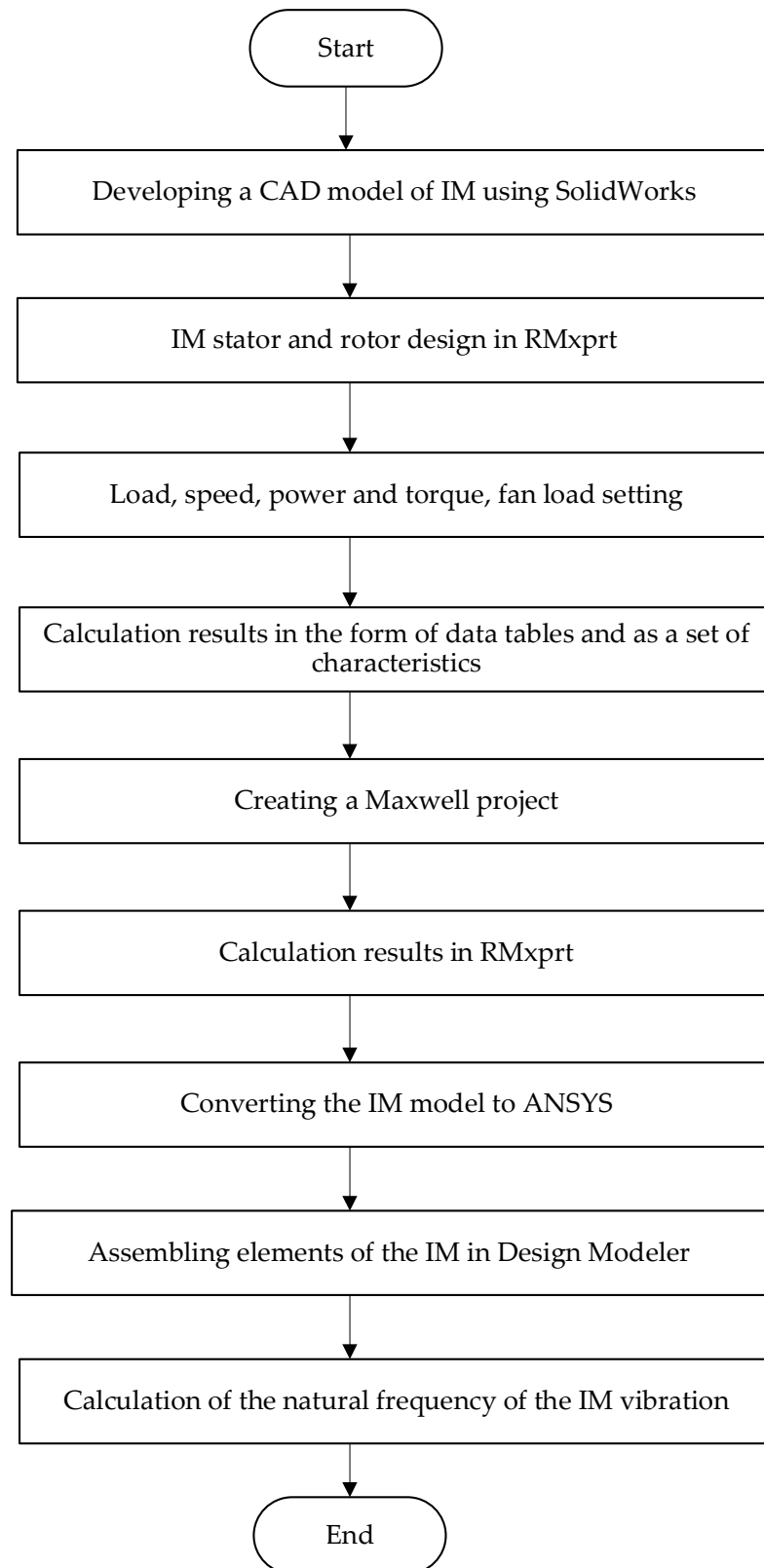


Figure 1. A diagram of the information flow of the design of the IM.

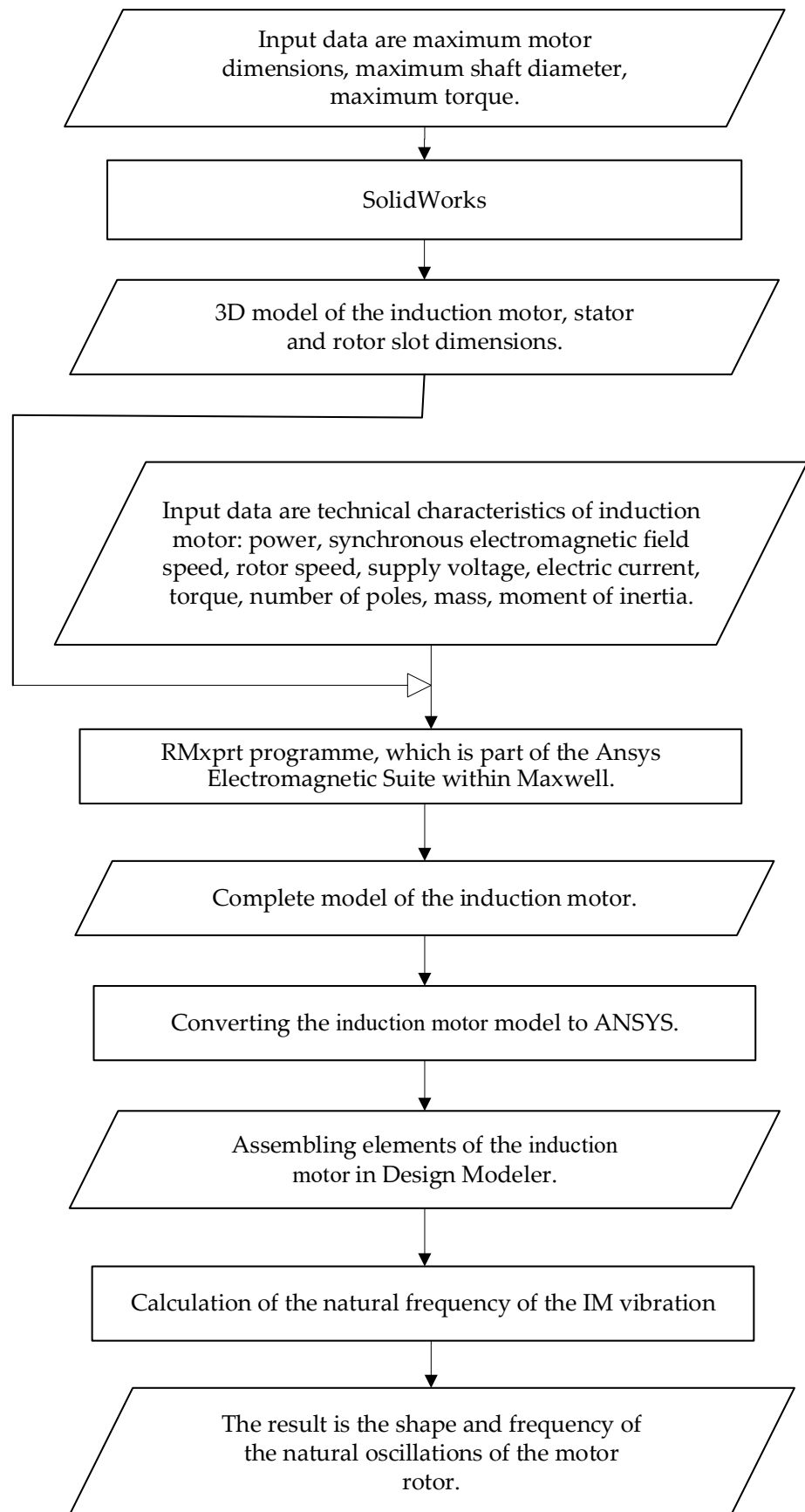


Figure 2. A diagram of information flow when designing the asynchronous motor.

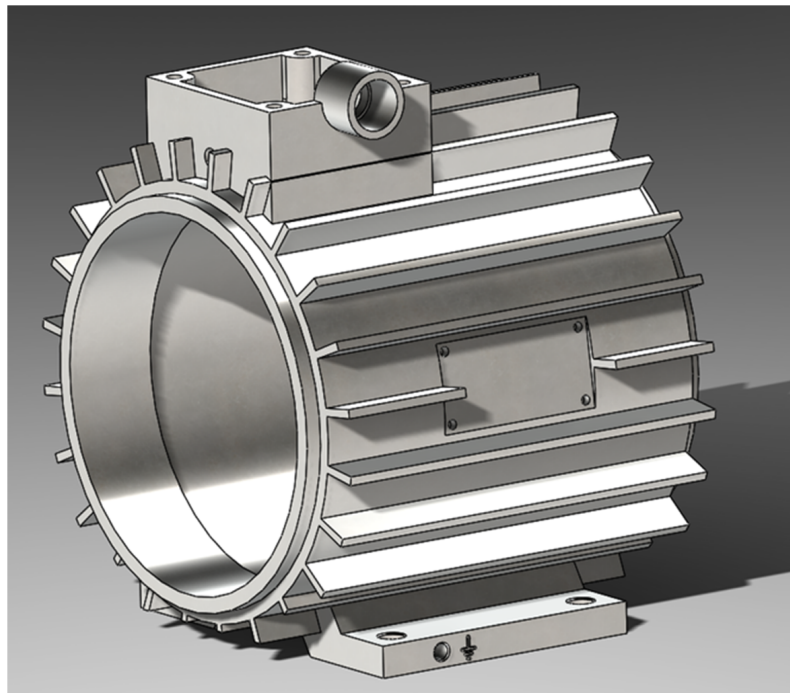


Figure 3. SolidWorks. Induction motor enclosure.

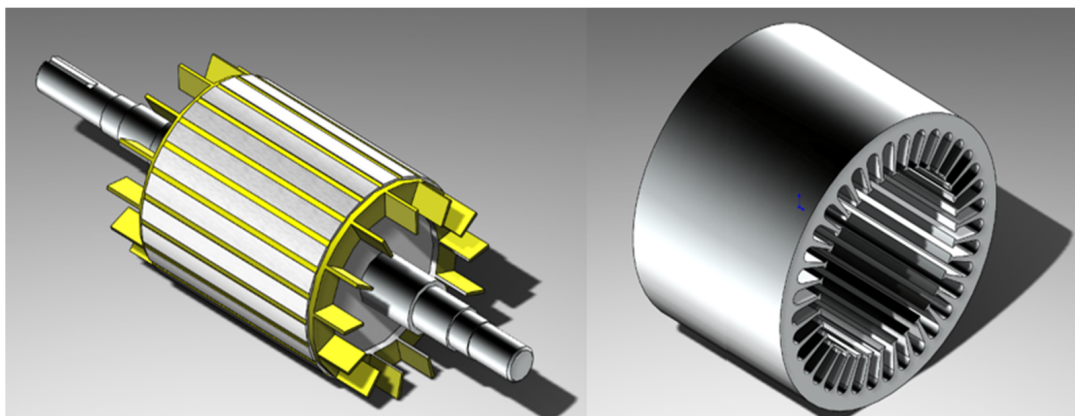


Figure 4. SolidWorks. Rotor and stator of induction motor.

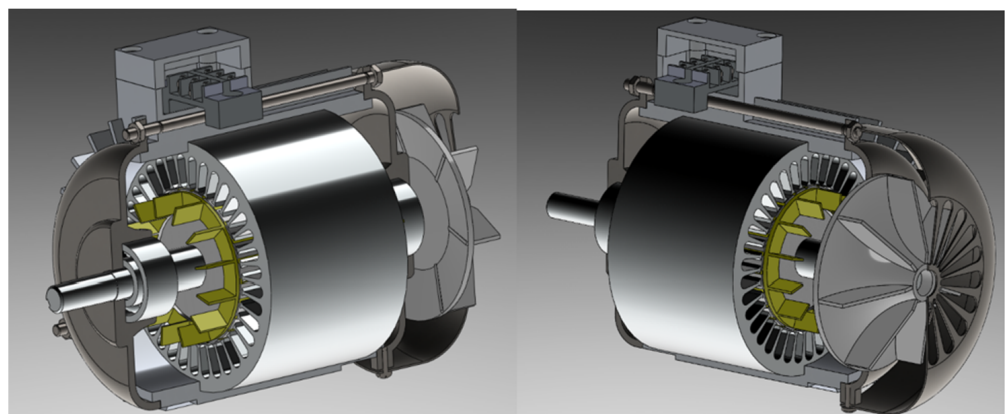


Figure 5. SolidWorks. Induction motor in sectional view.

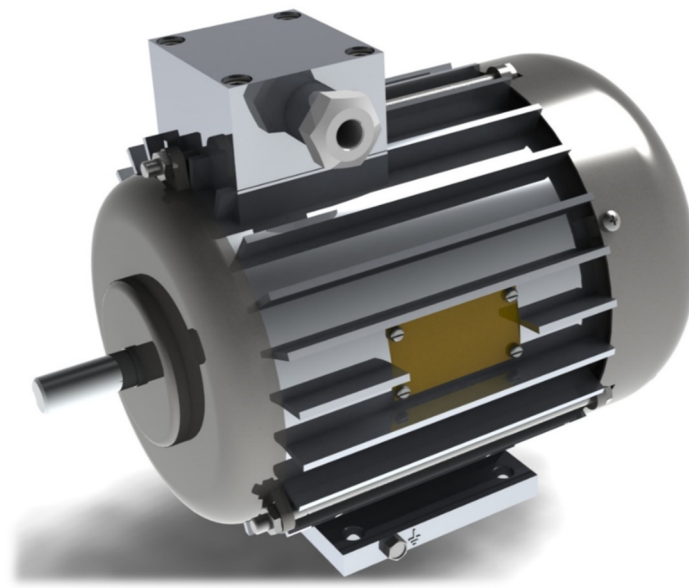


Figure 6. SolidWorks. 3D model of an induction motor AIR 63V2.

The finite element method (FEM) is a numerical approach utilized to solve partial differential equations and integral equations that arise in a wide range of applied physics problems. It has proven to be an effective technique in the fields of solid mechanics, heat transfer, fluid dynamics, and electrodynamics. The method involves dividing the domain where the differential equations need to be solved into a finite number of subdomains or elements. Each element is selected based on the characteristics of the problem being studied. Within each element, an approximation function is chosen, often in the form of a polynomial of the first degree for the simplest case. The selection of these approximation functions is arbitrary and may differ for each element.

When the approximating function is evaluated outside of its designated range, it evaluates to zero. The values of the function at the boundary nodes, which represent the solution to the problem, are not known beforehand. Typically, the coefficients of the approximating functions are determined by enforcing the equality of neighboring function values at the nodes that define the boundaries between elements. These coefficients are then expressed in terms of the function values at the nodes within each element.

A set of linear algebraic equations is constructed with the number of equations directly proportional to the number of unknown values at nodes where the solution is sought. This number is limited only by the computer's capabilities and is determined by the number of elements. As each element is only related to a limited number of neighboring elements, the resulting system of equations is sparse, making it much easier to solve.

In matrix terms, stiffness and mass matrices (also known as Dirichlet matrices) are assembled. Boundary conditions are then applied to these matrices, such as Neumann conditions that leave the matrices unchanged or Dirichlet conditions that remove rows and columns corresponding to boundary nodes where the solution components are already known. The system of linear equations is then constructed and solved using some of the known methods [30].

The application of the method in electrodynamics is based on Maxwell's equations, which are formulated as follows.

Gauss's law:

$$\oint D ds = Q, \quad (1)$$

where D is the flux of electric field strength through a closed surface, s is the surface area, and Q is the charge enclosed within that surface.

Gauss's law for the magnetic field:

$$\oint \mathbf{B} ds = 0, \quad (2)$$

where \mathbf{B} is the flux of the magnetic induction vector through any closed surface.

Faraday's law of induction:

$$\oint \mathbf{E} dl = -\frac{d}{dt} \int \mathbf{B} ds, \quad (3)$$

where \mathbf{E} is the electric vector field, and dl is an infinitesimal vector element of the contour.

Biot–Savart–Laplace law:

$$\oint \mathbf{H} dl = I + \frac{d}{dt} \int \mathbf{D} ds, \quad (4)$$

where \mathbf{H} is the magnetising force or magnetising, I is electric current, and \mathbf{D} is electric induction.

Additional relations:

$$\mathbf{B} = \mu \mu_0 \mathbf{H}, \quad (5)$$

where μ is the property of the magnetic material called its permeability, and μ_0 is the magnetic constant or the permeability of free space, is the proportionality between magnetic induction and magnetizing force when forming a magnetic field in a classical vacuum.

$$\mathbf{D} = \varepsilon \varepsilon_0 \mathbf{E}, \quad (6)$$

where ε is relative permittivity, and ε_0 is dielectric constant.

$$\mathbf{j} = \sigma \mathbf{E}, \quad (7)$$

where \mathbf{j} is free charge current density, and σ is specific conductivity.

Equations (1)–(7) are utilized as a basic principle for the calculations in the Maxwell software, which utilizes the finite element method (FEM) to accurately compute static, harmonic electromagnetic and electric fields, as well as transients in electric motors. These equations are not utilized for optimization purposes but rather to calculate the electrodynamics of an induction motor using the finite element method. The computation starts with the creation of a new project, wherein the category of electrical machine to be evaluated is explicitly stated (see Figure 7). Within the project manager, four classifications materialize in the established project: machine, which pertains to the configuration of model parameters; analysis, which relates to the establishment of model calculation; optimetrics, which involves the determination of model optimization parameters; and results, which deals with the output of analysis findings. The preliminary data for the IM AIR 63V2 motor is then introduced into the project. By utilizing a previously generated 3D model via the SolidWorks software, the dimensions of the stator and rotor slots are entered into the graphs. Unlike the 3D model, the simplification of the stator winding is deemed inadmissible in this computation.

Upon completion of the parameter input, a symbolic representation of the object under examination will be displayed on the screen (see Figures 8 and 9).

Following the completion of the RMXprt forms, the project will be prepared for computation. A new solution profile will be generated, and solution parameters, such as various load types (e.g., constant speed, power, torque, and fan load), will be entered [31]. Figure 10 presents the Solution Profile window.

The subsequent step involves verifying and computing the project. The computation results will be presented in two formats: as data tables and as a set of characteristics. Figure 10 illustrates the Project Calculation Result window in tabular form, while another view of the Project Calculation Result window as a feature is shown in Table 1.

Table 1 shows the torque calculation with locked rotor (2.564 Nm), stator winding electric current with locked rotor (0.35 mA), stator winding resistance (0.48 Ohm), and rotor resistance (0.34 Ohm).

Figure 11 presents a graph of the change in electromagnetic torque as a function of the slip value. It is shown that the maximum torque corresponds to a slip of 0.18–0.2.

The creation of the Maxwell project is accomplished automatically, resulting in a complete IM model for research purposes. A 3D project of the IM is presented in Figure 12.

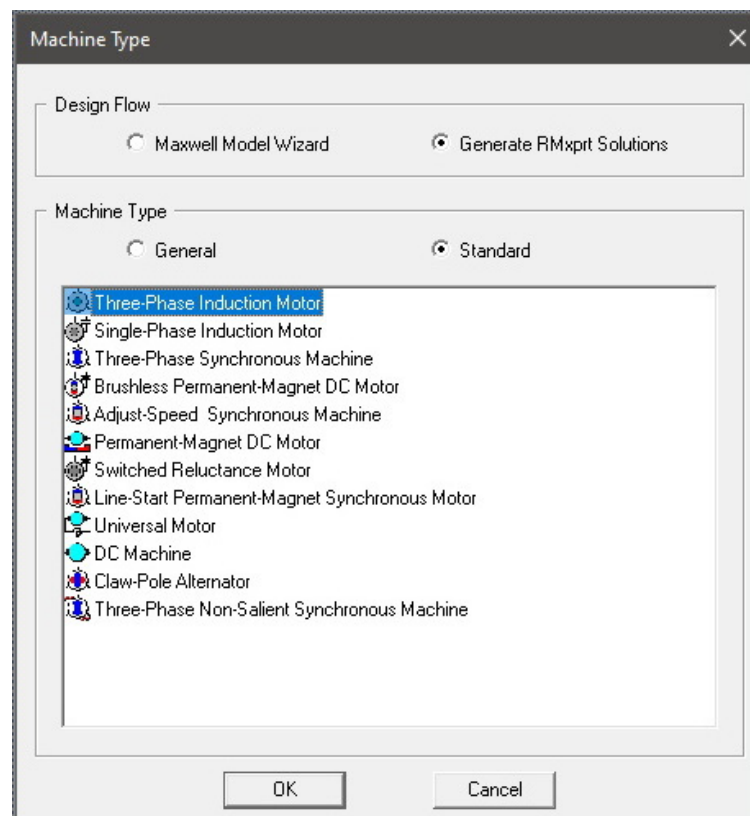


Figure 7. Selecting the type of electric motor.

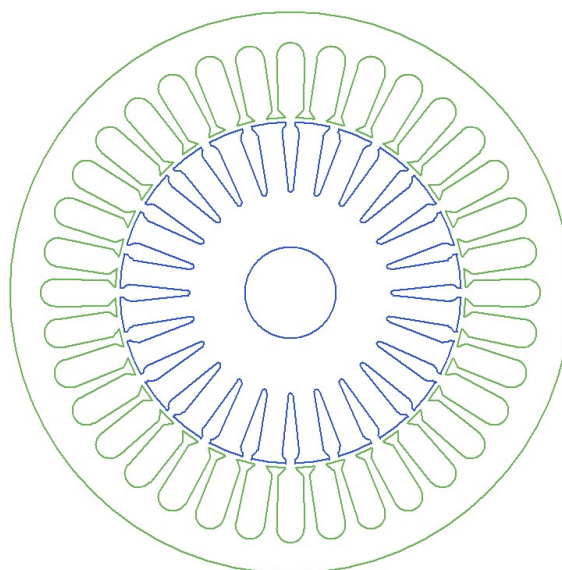


Figure 8. Stator and rotor in RMxprt.

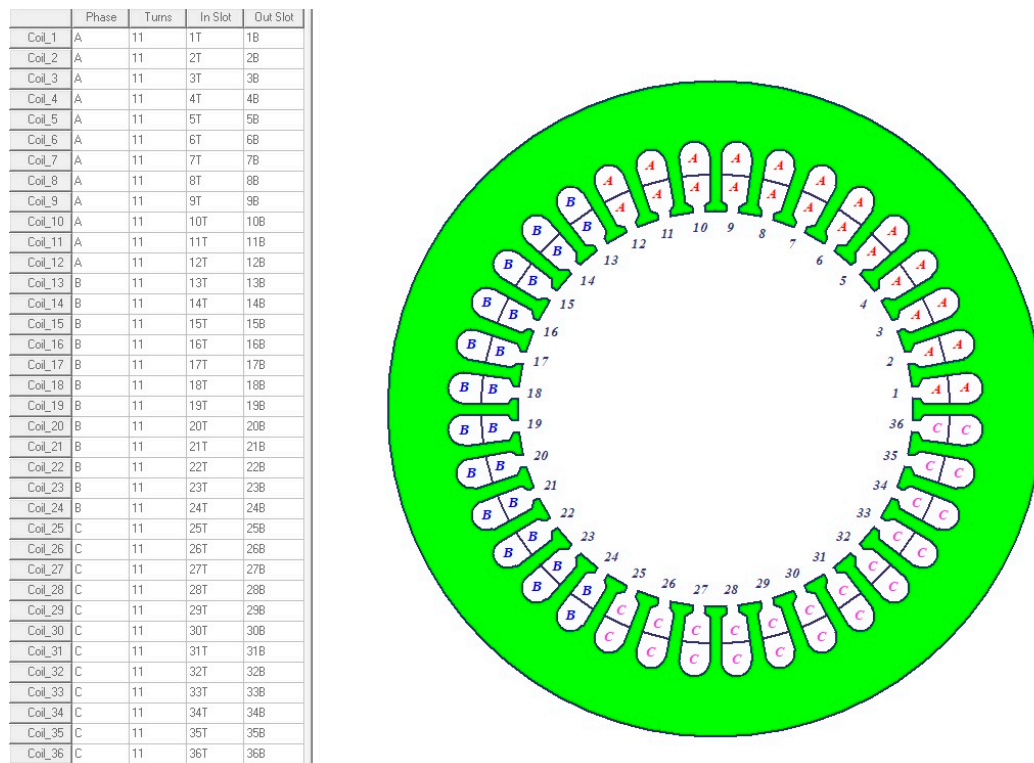


Figure 9. End connections in stator winding.

Properties: Project1 - RMxprtDesign1

General | IndM3

Name	Value	Unit	Evaluated Value	Description	Read-only
Name	Setup1				<input type="checkbox"/>
Enabled	<input checked="" type="checkbox"/>				<input type="checkbox"/>
Operation Type	Motor			Motor or generator	<input checked="" type="checkbox"/>
Load Type	Const Power			Mechanical load type	<input type="checkbox"/>
Rated Output ...	0.55	kW	0.55kW	Rated mechanical or el...	<input type="checkbox"/>
Rated Voltage	380	V	380V	Applied or output rated ...	<input type="checkbox"/>
Rated Speed	2770	rpm	2770rpm	Given rated speed	<input type="checkbox"/>
Operating Tem...	75	cel	75cel	Operating temperature	<input type="checkbox"/>

☐ Show Hidden

OK Отмена Применить

Figure 10. Solution Profile window.

Table 1. Project calculation result window in tabular form.

	Name	Value	Units
1.	Locked Rotor Torque	2.564	NewtonMeter
2.	Locked Rotor Phase Current	0.35038	mA
3.	Locked Rotor Torque Ratio	0.31969	
4.	Locked Rotor Current Ratio	3.09272	
5.	Stator Resistance	0.481065	ohm
6.	Stator Leakage Reactance	0.726126	ohm
7.	Rotor Resistance	0.339619	ohm
8.	Rotor Leakage Reactance	0.698721	ohm

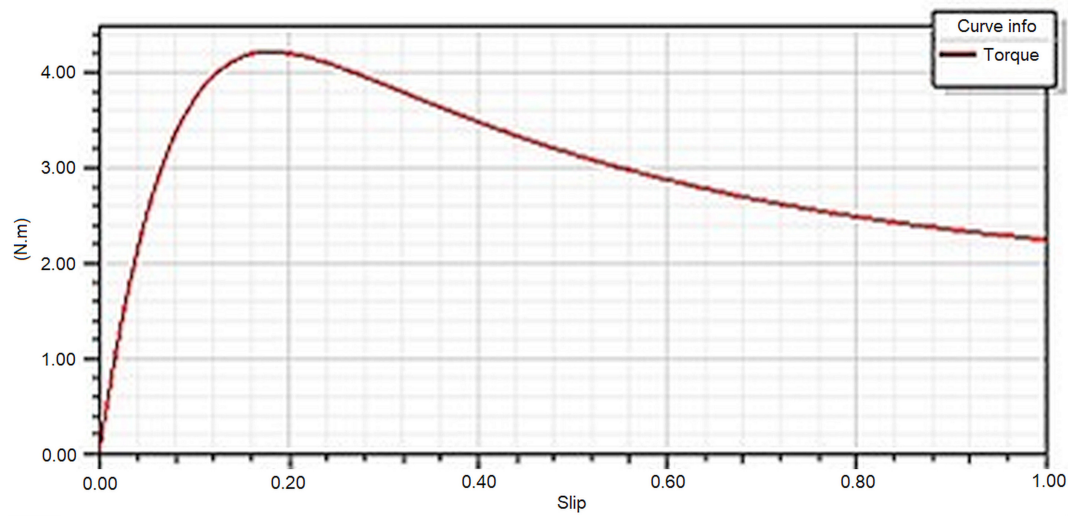


Figure 11. Torque vs Slip project Calculation Result window as a feature.

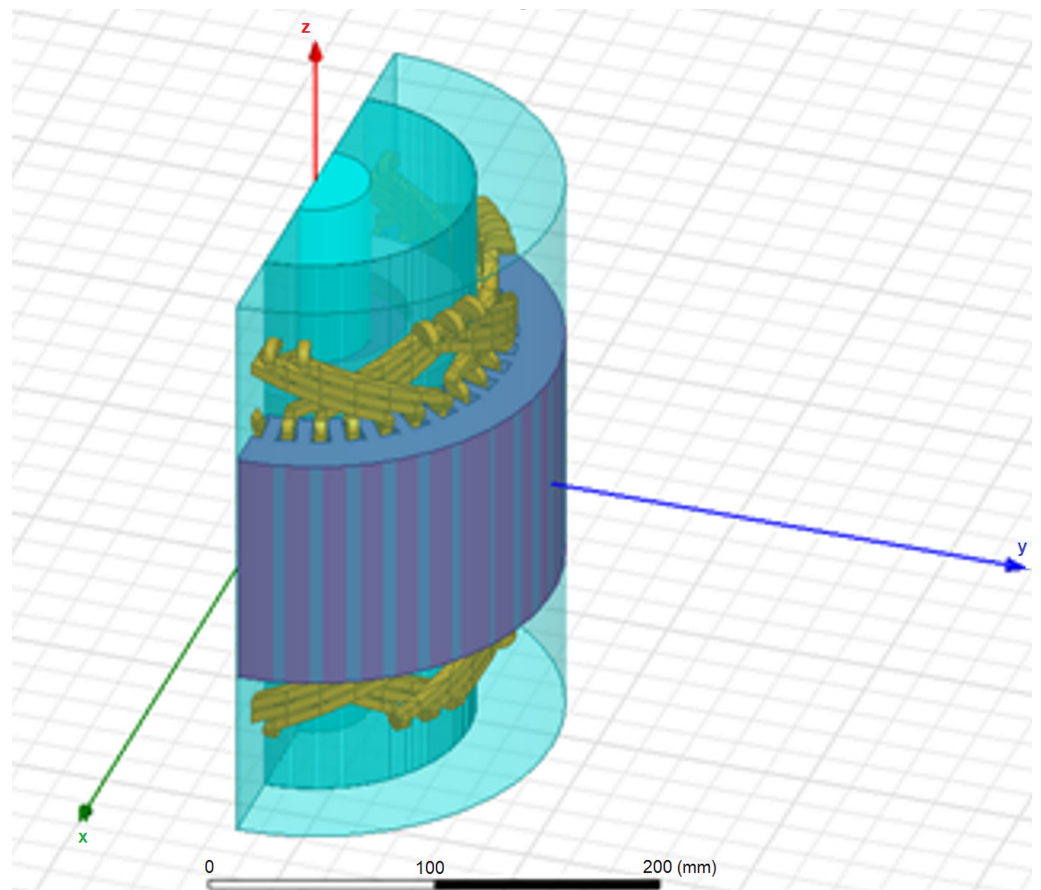


Figure 12. Automatically generated Maxwell 3D project.

3. Results

The RMxpert calculation results in the following data:

Rated current: $I = 1.57 \text{ A}$

Nominal torque: $M = 1.69 \text{ N}\cdot\text{m}$

Nominal speed: 2650 rpm

Based on the data, it can be concluded that the calculations performed with the RMxpert software were accurate. In future investigations of the dynamics of induction motors using

this design, various parameters can be modified efficiently, leading to the determination of values optimized for a particular condition.

The investigation of the dynamics of the system of moving elements of an asynchronous motor is crucial due to its significant impact on the vibration state of the entire motor. The dynamic properties of the whole machine play a vital role during the development of the motor parameterization test bench. The natural vibrations of the structure are calculated to prevent the operating frequencies from aligning with the resonance frequencies.

The purpose of this calculation is to conduct a modal analysis of the motor rotor in conjunction with other moving elements of the system while accounting for the gyroscopic effect. A complete CAD model of the induction motor, utilizing finite element analysis, has been generated. The first step of the calculation involves converting the necessary elements into the Ansys software. Figure 13 displays the CAD model in the SolidWorks software.

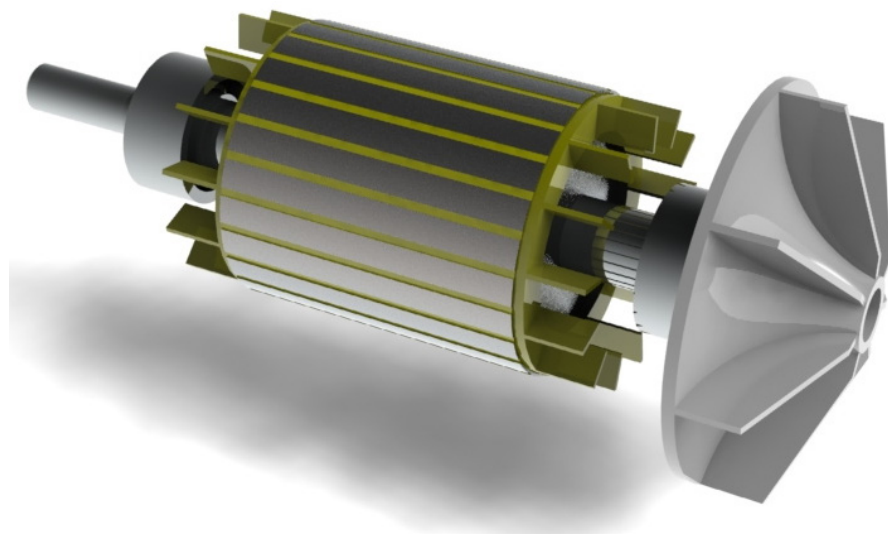


Figure 13. CAD model in SolidWorks software.

Imported objects include motor rotor, impeller, and two bearings 6201 ZZ-C3. Figure 14 shows assembling imported models in Ansys—Design Modeler.

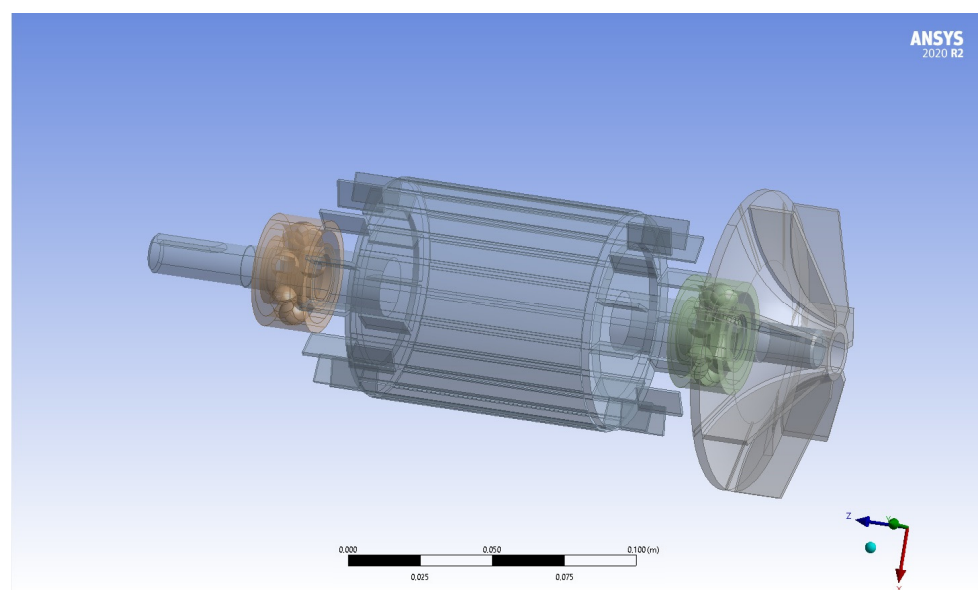


Figure 14. Assembling imported models in Ansys—Design Modeler.

When importing files in .step or .parasolid format, a problem may arise such as artifacts on the edges of circles, overhangs, and roundings. To solve these problems, the original geometry must be corrected. To accomplish this, a body operation element is created on the Create tab, and Simplify is selected on the type table. All assembly elements are then marked and renamed according to their purpose. This completes the part preparation for calculations. Figure 15 shows avoiding artefacts on parts.

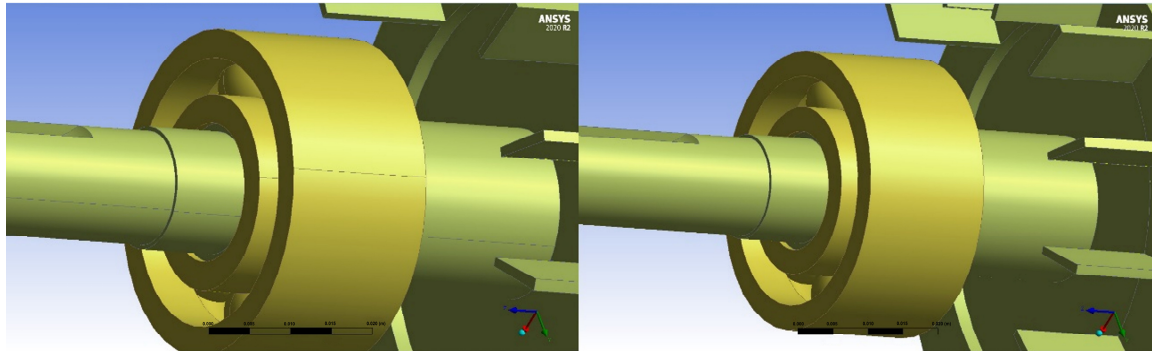


Figure 15. Avoiding artefacts on parts.

Materials must be assigned to all components. The rotor, which is a composite part, will include several materials. The bearing material will be assigned according to the bearing datasheet of the medium series, and the shaft material will be assigned according to the motor datasheet. The impeller will be assigned polycapromide.

Contact surfaces are then checked or assigned. As the rotor is a single construction, there will be no contact surface assignment to the shaft. This is not a critical aspect since the entire rotor will be calculated as one unit. Figure 16 shows assigning contact surfaces.

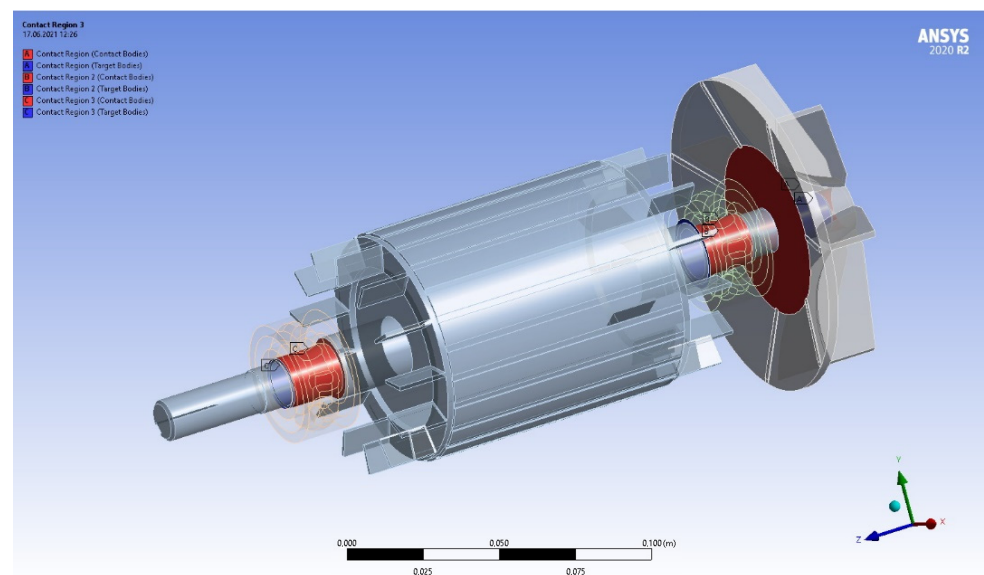


Figure 16. Assigning contact surfaces.

The next step is to create a mesh of objects to investigate. The more precise the polygonal mesh, the more accurate the calculation will be, but the more processing power it will require. Attention must be paid to element joints, rounded surfaces, and surfaces with complex geometry to make local adjustments to the mesh and avoid interference. Figure 17 shows creating a polygonal mesh of objects.

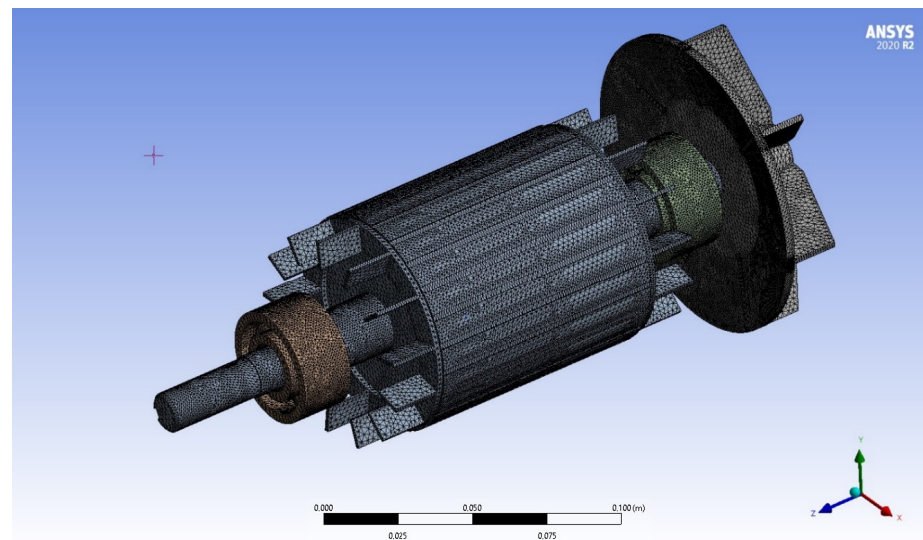


Figure 17. Creating a polygonal mesh of objects.

After defining and editing the mesh, it is necessary to establish boundary conditions by setting rigid terminations on the raceways of the inner rings of the bearings.

Rotor dynamics simulations can be conducted in two different reference systems: stationary and rotating. Ansys considers the gyroscopic effect by using a damping matrix, where a negative value represents a stable oscillation form, and a positive value corresponds to an unstable one. The imaginary part indicates the natural frequency, including damping. Despite using a damping matrix to account for the gyroscopic effect, no energy dissipation occurs in the absence of specified damping in the model. Thus, all real parts of complex frequencies are set to zero.

To initiate the calculation, one needs to select Solve from the context menu of the modal item. Upon successful completion of the computation, a green check mark will appear in the project tree, and the graphic window will display an armature shape deformed according to its frequency, specified in the mode cell of the parameter panel.

The result obtained in the fixed reference frame indicates a frequency range of 922 to 1015 Hz. Figure 18 presents the Ansys calculation result.

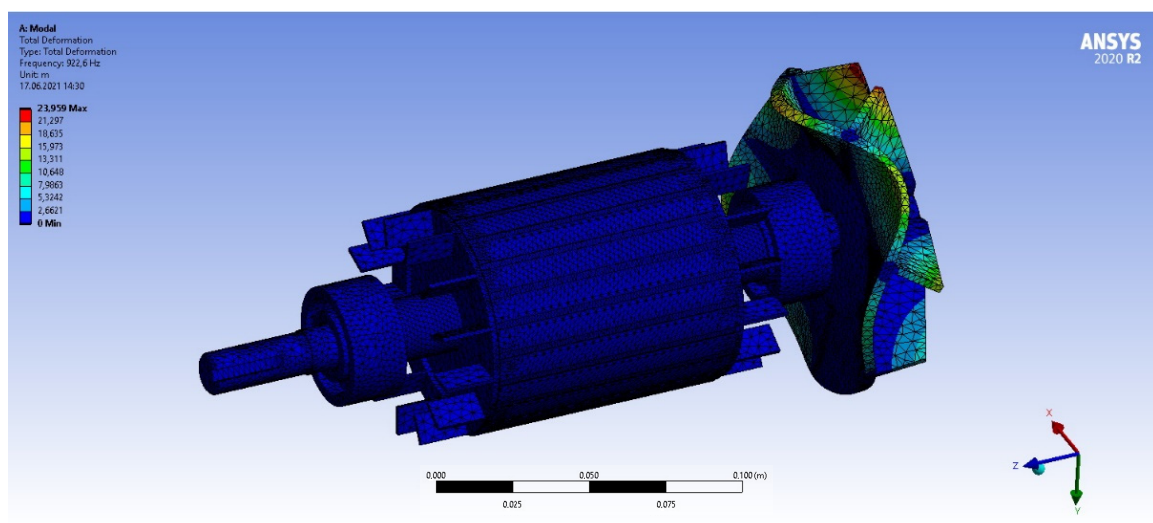


Figure 18. Ansys calculation result, the legends of total deformation, micrometer: 21.297; 18.635; 15.973; 13.311; 10.648; 7.9863; 5.3242; 2.6621; 0.

The animation tools available in the mechanical package enable the visualization of natural vibration patterns. It should be noted that the natural frequency of the IM rotor ranges from 922 Hz to 1015 Hz. Consequently, for the given configuration, frequencies within this range should be excluded when preparing the control regimes for the IM of the given configuration. The aforementioned calculation does not account for mounting and thermal stresses, gas forces, and temperature-induced changes in material properties.

4. Discussion

Using the performance of the developed model, the time dependence of electromagnetic torque of the IM was obtained from the mathematical model. These data facilitate the observation of the motor's state at predetermined time points. The developed mathematical model can be used to adjust data for any IM configuration and to perform further calculations to generate dependency graphs.

The Ansys software was utilized to experimentally acquire various data that directly affect motor performance and control.

By modifying the internal winding components and stator and rotor designs, the resulting current, torque, and operating speeds can be adjusted. Conversely, in the case of any deviations in the real motor, faults can be observed in relation to the real readings and the readings that have been calculated in the Ansys software.

The natural vibration calculations of the CAD model of the IM can serve as a starting point for technical diagnostics of the motor [32]; however, modifications to the real IM, such as changes in air gap or rotor eccentricity, can significantly change the readings, potentially leading to a decrease in the operating frequency range and a negative impact on overall motor performance [33].

When investigating the drive for the potential usage in robots and manipulators, additional values can be incorporated into all models, including those with gearboxes, to monitor available parameters [34]. In case of unfavorable results, adjustments can be made to the equipment to ensure optimal engine performance.

5. Conclusions

A computer model of an induction motor has been developed to facilitate the generation of design documentation and control programs for CNC tools to manufacture motor components or conduct further research. A CAD model of the motor was constructed in the SolidWorks software based on of the existing AIR63V2 motor in order to conduct finite element analysis. The motor's housing, rotor, and stator were designed, and its electrical parameters were calculated in Ansys Electronic Suite—Maxwell RMxpert, using classical analytical theory of electrical machines and the equivalent magnetic circuit method.

The calculations take into account various factors, such as the non-linearity of electrical steel, the non-sinusoidality of the magnetic flux in the gap, and the displacement of electric current in massive conductors. A complete model of the induction motor for research purposes was generated, and the speed and electromagnetic torque dependencies were obtained.

The natural frequency of the rotor was calculated to be between 922 Hz and 1015 Hz, and these values of natural oscillations of the CAD model of the motor can be used for the motor diagnostics. The model created in Ansys can be used to design an IM with specific characteristics, optimized for the required tasks. Results of investigations presented herein can be adapted and employed for the purpose of examining IMs with differing parameters.

Author Contributions: Conceptualization, P.B. and T.K.; methodology, P.B. and T.K.; software, V.P.; validation, P.B., T.K. and V.P.; formal analysis, P.B. and T.K.; investigation, P.B., T.K. and V.P.; resources, V.P.; data curation, P.B., T.K. and V.P.; writing—original draft preparation, P.B. and T.K.; writing—review and editing, T.K. and V.P.; visualization, T.K. and V.P.; supervision, T.K. and V.P.; project administration, P.B. and V.P.; funding acquisition, P.B. All authors have read and agreed to the published version of the manuscript.

Funding: This work was funded by the Ministry of Education, Science, Research and Sport of the Slovak Republic within projects KEGA 006STU-4/2021, VEGA No. 1/0823/21, and KEGA 001STU-4/2022.

Institutional Review Board Statement: Not applicable.

Informed Consent Statement: Not applicable.

Conflicts of Interest: The authors declare no conflict of interest. The funders had no role in the design of the study; in the collection, analyses, or interpretation of data; in the writing of the manuscript; nor in the decision to publish the results.

References

1. Hameyer, K.; Belmans, R. *Numerical Modelling and Design of Electrical Machines and Devices*; WIT Press: Billerica, MA, USA, 1999; 340p, ISBN 1-85312-626-8.
2. Boldea, I. *Induction Machines Handbook: Transients, Control Principles, Design and Testing*; CRC Press: Boca Raton, FL, USA, 2020; 455p, ISBN 978-0-367-46618-3.
3. Boldea, I.; Tutelea, L.N. *Electric Machines: Transients, Control Principles, Finite Element Analysis, and Optimal Design with MATLAB*, 2nd ed.; CRC Press, Taylor & Francis Group: Boca Raton, FL, USA, 2022; 455p, ISBN 9780367375652.
4. Krenicky, T.; Nikitin, Y.; Božek, P. Model-Based Design of Induction Motor Control System in MATLAB. *Appl. Sci.* **2022**, *12*, 11957. [\[CrossRef\]](#)
5. Kumar, L.A.; Alexander, S.A.; Maheswari, Y.U. *Design and Simulation of Electrical Machines with Matlab*; Nova Science Publishers: New York, NY, USA, 2022; 272p.
6. Crowder, R. *Electric Drives and Electromechanical Systems: Applications and Control*, 2nd ed.; Butterworth-Heinemann: Oxford, UK, 2020; 309p, ISBN 978-0-08-102884-1.
7. Peterka, J.; Pokorný, P.; Vaclav, S. CAM strategies and surfaces accuracy. In *Annals of DAAAM for 2008, Proceedings of the 19th International DAAAM Symposium, Trnava, Slovakia, 22–25 October 2008*; Book Series: Annals of DAAAM and Proceedings; DAAAM International Vienna: Wien, Austria, 2008; pp. 1061–1062.
8. Peterka, J.; Senderska, K.; Vaclav, S.; Pokorný, P. Product design suitable for assembly. In *Annals of DAAAM for 2008, Proceedings of the 19th International DAAAM Symposium, Trnava, Slovakia, 22–25 October 2008*; Book Series: Annals of DAAAM and Proceedings; DAAAM International Vienna: Wien, Austria, 2008; pp. 1063–1064.
9. Jakubowski, J.; Peterka, J. Design for manufacturability in virtual environment using knowledge engineering. *Manag. Prod. Eng. Rev.* **2014**, *5*, 3–10. [\[CrossRef\]](#)
10. El-Sharkawi, M.A. *Fundamentals of Electric Drives*, 2nd ed.; Cengage Learn: Boston, MA, USA, 2019; 364p, ISBN 978-1-305-97096-0.
11. Gurocak, H. *Industrial Motion Control: Motor Selection, Drives, Controller Tuning, Applications*; Wiley: Hoboken, NJ, USA, 2015; 320p.
12. Hughes, A.; Drury, B. *Electric Motors and Drives: Fundamentals, Types and Applications*, 5th ed.; Newnes: Oxford, UK, 2019; 495p, ISBN 978-0-08-102615-1.
13. Sang-Hoon, K. *Electric Motor Control: DC, AC, and BLDC Motors*; Elsevier Science: Amsterdam, The Netherlands, 2017; 438p, ISBN 978-0128121382.
14. Shaitor, N.M.; Yakimovich, B.A.; Gorpichenko, A.V.; Solomennikova, S.I. Influence of Thermal and Electromagnetic Processes in Double-Layer Rotors on the Efficiency of Asynchronous Motors. *Vestn. IzhGTU Im. M.T. Kalashnikova* **2021**, *24*, 114–123. [\[CrossRef\]](#)
15. Shaytor, N.M.; Gorpichenko, A.V. Dynamic Modes of Asynchronous Motors in Drives of Power Systems and Complexes. *Vestn. IzhGTU Im. M.T. Kalashnikova* **2020**, *23*, 95–101. (In Russian) [\[CrossRef\]](#)
16. Le Roux, P.F.; Ngwenyama, M.K. Static and Dynamic Simulation of an Induction Motor Using Matlab/Simulink. *Energies* **2022**, *15*, 3564. [\[CrossRef\]](#)
17. Wang, X.; Palka, R.; Wardach, M. Nonlinear Digital Simulation Models of Switched Reluctance Motor Drive. *Energies* **2020**, *13*, 6715. [\[CrossRef\]](#)
18. Mao, X.; Chen, J. A Fast Method to Compute the Dynamic Response of Induction Motor Loads Considering the Negative-Sequence Components in Stability Studies. *Energies* **2019**, *12*, 1802. [\[CrossRef\]](#)
19. Oluic, M.; Ghandhari, M.; Berggren, B. Methodology for rotor angle transient stability assessment in parameter space. *IEEE Trans. Power Syst.* **2017**, *32*, 1202–1211.
20. Pati, S.; Choudhury, A.; Gantayat, J. An Estimation-Based Sliding Mode Control Structure for High-Performance Control of Induction Motor. In *Smart Technologies for Power and Green Energy*; Lecture Notes in Networks and Systems; Dash, R.N., Rathore, A.K., Khadkikar, V., Patel, R., Debnath, M., Eds.; Springer: Singapore, 2023; Volume 443. [\[CrossRef\]](#)
21. Goolak, S.; Gubarevych, O.; Yermolenko, E.; Slobodyanyuk, M.; Gorobchenko, O. Mathematical modeling of an induction motor for vehicles. *East. Eur. J. Enterp. Technol.* **2020**, *2*, 104. [\[CrossRef\]](#)
22. Khamsehchi, S.; Mölsä, E.; Hinkkanen, M. Comparison of standstill parameter identification methods for induction motors. In *Proceedings of the IEEE 9th International Symposium on Sensorless Control for Electrical Drives (SLED)*, Helsinki, Finland, 13–14 September 2018; pp. 156–161.

23. Liu, Y.; Bazzi, A.M. A detailed induction machine core loss model in the arbitrary reference frame. In Proceedings of the IEEE Applied Power Electronics Conference and Exposition (APEC), Charlotte, NC, USA, 15–19 March 2015; pp. 2617–2622.
24. Panwar, V.; Varma, H.; Rawat, S.; Pant, P.; Banerjee, S.; Sharma, S. Dynamic model of 3-phase induction motor for control utilities. *J. Inf. Optim. Sci.* **2022**, *43*, 245–249. [[CrossRef](#)]
25. Li, Z.; Guo, P.; Han, R.; Wang, Q. Torque modeling and characteristic analysis of electromagnetic piezoelectric hybrid-driven 3-degree-of-freedom motor. *Adv. Mech. Eng.* **2018**, *10*, 1–15. [[CrossRef](#)]
26. Nikitin, Y.; Krenický, T.; Božek, P. Diagnostics of automated technological drives. In *Monitoring and Analysis of Manufacturing Processes in Automotive Production*; RAM-Verlag: Lüdenscheid, Germany, 2022; Volume 6, 148p, ISBN 978-3-96595-018-4.
27. Stollmann, V.; Nikitin, Y.R.; Shoshin, A.O. RELAZ Devices. *Vestn. IzhGTU Im. M.T. Kalashnikova* **2022**, *25*, 79–88. [[CrossRef](#)]
28. Kuric, I.; Nikitin, Y.; Sága, M.; Tlach, V.; Bannikov, A. Development of Electric Drive on the Basis of Five-Phase Synchronous Electric Motor. *Electronics* **2022**, *11*, 2680. [[CrossRef](#)]
29. Božek, P.; Krenický, T.; Stepanov, P.; Nikitin, Y.; Gupalov, B.; Lagutkin, S. Development of a System for Predictive Diagnostics of Traction Asynchronous Electric Drive for Trains. *MM Sci.* **2022**, *4*, 6123–6126.
30. Božek, P.; Nikitin Yu Krenický, T. Methods, Models, Algorithms for Diagnostics of Mechatronic Systems. In *Diagnostics of Mechatronic Systems*; Studies in Systems, Decision and Control; Springer: Cham, Switzerland, 2021; Volume 345, pp. 17–26.
31. Kuric, I.; Klačková, I.; Nikitin, Y.R.; Zajačko, I.; Cisar, M.; Tucki, K. Analysis of diagnostic methods and energy of production systems drives. *Processes* **2021**, *9*, 843. [[CrossRef](#)]
32. Cheng, C.; Wang, Q.; Nikitin, Y.; Liu, C.; Zhou, Y.; Chen, H. A data-driven distributed fault detection scheme based on subspace identification technique for dynamic systems. *Int. J. Robust Nonlinear Control.* **2022**, *33*, 3107–3128. [[CrossRef](#)]
33. Sága, M.; Vasko, M.; Handrik, M.; Kopas, P. Contribution to random vibration numerical simulation and optimisation of nonlinear mechanical systems. *Sci. J. Sil. Univ. Technol. Ser. Transp.* **2019**, *103*, 143–154. [[CrossRef](#)]
34. Kopas, P.; Sága, M.; Baniari, V.; Vasko, M.; Handrik, M. A plastic strain and stress analysis of bending and torsion fatigue specimens in the low-cycle fatigue region using the finite element methods. *Procedia Eng.* **2017**, *177*, 526–531. [[CrossRef](#)]

Disclaimer/Publisher's Note: The statements, opinions and data contained in all publications are solely those of the individual author(s) and contributor(s) and not of MDPI and/or the editor(s). MDPI and/or the editor(s) disclaim responsibility for any injury to people or property resulting from any ideas, methods, instructions or products referred to in the content.